Analysis of a heterodyne-detected transient-grating experiment on a molecular supercooled liquid. II. Application to m-toluidine

Analysis of a heterodyne-detected transient-grating experiment on a molecular supercooled liquid. II. Application to *m*-toluidine

A. Azzimani, C. Dreyfus, and R. M. Pick
IMPMC, Université P. et M. Curie et CNRS-UMR 7590, F-75015 Paris, France

P. Bartolini, A. Taschin, and R. Torre
LENS and Dipartimento di Fisica, Università di Firenze, I-50019 Sesto Fiorentino, Italy
and INFM-CRS-Soft Matter (CNR), c\o Università la Sapienza, Italy

(Received 20 February 2007; published 24 July 2007)

This paper reports the first detailed analysis of a transient grating (TG) experiment on a supercooled molecular liquid, *m*-toluidine, from 330 K ($1.75T_g$) to 190 K ($1.01T_g$) based on the theoretical model presented in Paper I of this series. This method allows one to give a precise description, over a wide dynamical range, of the different physical phenomena giving rise to the signals. Disentangling the isotropic and the anisotropic parts of the TG response, a careful fitting analysis yields detailed information on the rotation-translation coupling function. We also extract the structural relaxation times related to the "longitudinal" viscosity over almost 10 decades in time and the corresponding stretching coefficient. The value of some other parameters and information on their thermal behavior is also reported.

DOI: 10.1103/PhysRevE.76.011510 PACS number(s): 64.70.Pf, 78.47.+p, 61.25.Em

I. INTRODUCTION

We present here the results of a heterodyne-detected transient-grating (HD-TG) experiment performed on *m*-toluidine and analyzed following the method proposed in Paper I [25] of this series. Three reasons led us to choose this substance as the first glassforming liquid composed of anisotropic molecules on which to test the applicability of this method.

First, *m*-toluidine is easy to supercool and to maintain in this state whatever the cooling rate and the temperature above its glass transition temperature, T_g=187 K [1]. Furthermore, the liquid phase exists in a large temperature domain, with a boiling temperature T_b=476 K [1(b)], is chemically stable, and is transparent once properly distilled.

Second, because of these properties, this supercooled phase has been already studied by various techniques such as dielectric measurements [2,3], optical Kerr effect (OKE) [4], molecular dynamics calculations with optimized potentials derived from first principles [5,6], light scattering spectroscopy [7], or frequency dependent specific heat measurements [3]. Some of those measurements provide us with the values and the thermal dependence of quantities which appear in the formulation of the theory. Their knowledge will help us in the analysis of the experiment.

Third, an HD-TG experiment had already been performed on this supercooled liquid [8]. It showed that the recorded signals depend only on the polarization of the probe and diffracted beams, provided that one limits the measurements to times longer than a few ns. This corresponds to the results given in the final part of Paper I which were derived under two conditions.

(1) The orientation of the molecules by the electric field of the pump beams can be neglected with respect to the two other sources (electrostriction and heat absorption) of the transient grating.

(2) One considers times long enough to neglect the OKE contribution, Eq. (2.9a) of Paper I, to the signals.

In that case, two and only two linearly independent signals can be extracted from measurements performed with different polarizations of the probe and detected beams; they do not depend on the polarization of the pump beams and two of their linear combinations, called the "iso" and the "aniso" signals, correspond, respectively, to the detection of the grating by the change in mass density and by the molecular orientation. When the pumps start to act at the time $t=-t_0$, these signals are expressed by

$$S_\alpha(\vec{q},t) = \frac{2}{\pi}\int_0^\infty \mathrm{Im}[S_\alpha(\vec{q},\omega)]\cos\,\omega(t+t_0)d\omega, \qquad (1.1)$$

where α stands either for "iso" or for "aniso," while $\vec{q}$ is the wave vector of the grating.

The expressions of $S_{\mathrm{iso}}(\vec{q},\omega)$ and $S_{\mathrm{aniso}}(\vec{q},\omega)$ which have to be used to fit the experimental signals for large enough values of $t+t_0$ were given by Eqs. (3.6) and (7) of Paper I and we reproduce them here. $S_{\mathrm{iso}}(\vec{q},\omega)$ is expressed as

$$S_{\mathrm{iso}}(\vec{q},\omega) = -I_{\mathrm{iso}}P_L(\vec{q},\omega)\left[\frac{1-\nu_\beta\omega g_\beta(\omega\tau_\beta)}{1+i\omega\tau_h(\vec{q},\omega)} - ia_0\right]F(\omega), \qquad (1.2)$$

where I_{iso} stands for an intensity. $S_{\mathrm{iso}}(\vec{q},\omega)$ depends, *inter alia*, on the heat diffusion time for wave vector $\vec{q}$ and frequency ω, $\tau_h(\vec{q},\omega)$, and on the phonon propagator, $P_L(\vec{q},\omega)$, that are given, Eqs. (3.8) and (3.13) of Paper I, by

$$\omega\tau_h(\vec{q},\omega) = \omega\tau_h^0(q)[1-\nu_{C_V}\omega g_{C_V}(\omega\tau_{C_V})], \qquad (1.3)$$

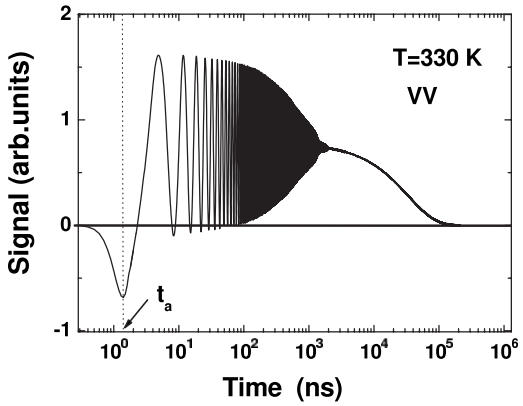

FIG. 1. VV signal at 330 K. Note the strong decrease of the phonon contribution in the 1–3 μs time range and the existence of negative parts of the signal for $t<30$ ps.

$$P_L^{-1}(\vec{q},\omega) = \omega^2 - q^2\left[c_a^2 + \Delta_L^2 \omega g_L(\omega\tau_L) + i\omega\bar{\gamma} + c_a^2\left(\frac{1}{\gamma} - 1\right)\frac{1}{1 + i\omega\tau_h(\vec{q},\omega)}\right]. \quad (1.4)$$

In Eq. (1.4), c_a is the adiabatic sound velocity, Δ_L is the amplitude of the term that couples c_a to the structural relaxation,[1] $\bar{\gamma}$ represents the contribution of the phonon anharmonicity to $P_L^{-1}(\vec{q},\omega)$, while γ is the usual ratio between the specific heats at constant pressure, C_P^{th}, and at constant volume, C_V^{th}, measured in a static experiment: γ is taken to be equal to unity in the adiabatic approximation of $P_L(\vec{q},\omega)$, and to its actual value in the isothermal form of the phonon propagator. Finally, whatever the index i, $g_i(\omega\tau_i)$ is the Laplace transform (LT) in the sense of Paper I, of a relaxation function $g_i(t/\tau_i)$ which has a value equal to 1 for $t=0$ and whose final decay (α-relaxation) is governed by the relaxation time τ_i. The index i stands for L, "longitudinal" relaxation process, in Eq. (1.4), and for C_V, specific heat at constant volume, in Eq. (1.3) where ν_{C_V} is the relative strength of the relaxation process contained in C_V^{th}:

$$\nu_{C_V} = \frac{\delta C_V^0}{C_V^{\text{th}}}, \quad (1.5)$$

where δC_V^0 is the difference between C_V^{th} and its instantaneous value. Furthermore, as all the signals that will be fitted correspond to the same wave vector $\vec{q}$, the q dependence will not be indicated anymore in $\tau_h^0(q)$ that will be simply written as τ_h^0.

The index i also corresponds to the thermal pressure function $\beta(\omega)$, in the numerator of the second bracket of Eq. (1.2): $g_\beta(\omega\tau_\beta)$ is the relaxation part of this function and ν_β its corresponding relative strength. Also, in the second half of the same bracket, a_0 represents the relative strength of the electrostriction source [ISBS contribution, Eq. (2.9c) of Paper I] with respect to the heat absorption source [ISTS contribution, Eq. (2.9b) of Paper I]. Finally, in the same equation, $F(\omega)$ is the LT of the response function of the whole HD-TG apparatus, the expression of $S_{\text{iso}}(\vec{q},\omega)$ implying that the pumps act during a time very short with respect to the time scale of $F(t)$.

[1] Δ_L is the quantity that relates the adiabatic sound velocity, c_a, also called the zero frequency sound velocity, c_0, to the infinite frequency sound velocity, c_∞, i.e., the sound velocity at frequencies higher than any relaxation frequency through $\Delta_L^2 = c_\infty^2 - c_0^2$.

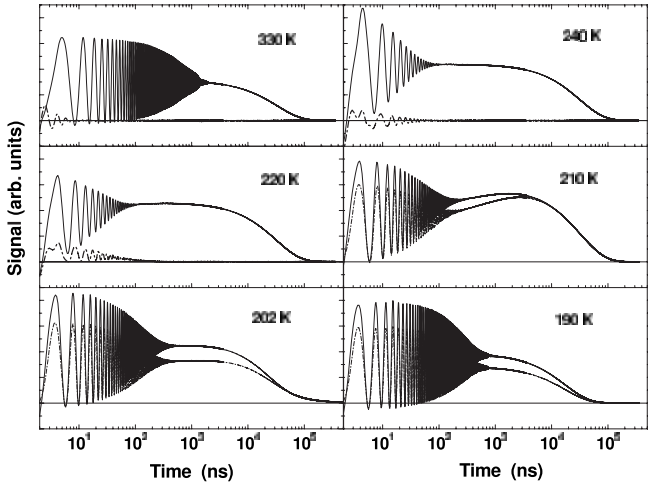

FIG. 2. VV (–) and HH (···) signals at six different temperatures. For the three highest temperatures, the dots (···) do not represent the HH signal but the difference between the VV and HH signals.

Similarly to Eq. (1.2), the anisotropic signal, $S_{\text{aniso}}(\vec{q},\omega)$, is expressed, see Eq. (3.9) of Paper I, as

$$S_{\text{aniso}}(\vec{q},\omega) = K_{\text{aniso}}[\omega g_\mu(\omega\tau_\mu) S_{\text{iso}}(\vec{q},\omega)]. \quad (1.6)$$

In this equation, K_{aniso} is the relative strength of the molecular orientation channel with respect to the mass density channel in the detection mechanism while $\omega g_\mu(\omega\tau_\mu)$ describes the relaxation process associated with the rotation-translation coupling.

The aim of this second paper is to use Eqs. (1.2) and (1.6) to fit, respectively, the isotropic and anisotropic signals of *m*-toluidine recorded between 330 and 195 K. All those fits will be performed in Sec. III and we shall discuss, in Sec. IV, the information so obtained. Before proceeding to those fits, we need to give, in Sec. II, some details on the experimental aspects of this work and to explain how we have obtained from previous experiments some of the parameters that appear in Eqs. (1.2)–(1.4).

II. EXPERIMENTAL ASPECTS

A. Presentation of the experimental results

The HD-TG *m*-toluidine signals were recorded from $t=-t_0$ to $t=0.5\times10^6$ ns with time steps equal to 100 ps up to $t=4$ μs, and to 8 ns afterwards, on the LENS instrument. This experimental setup is described in detail in [9], and [10] summarizes its latest modifications. A $S_{\text{VV}}^{\text{expt}}(\vec{q},t)$ signal, i.e., the signal measured with a V polarization of the probe and

TABLE I. Physical constants of *m*-toluidine.

Property	Value
Formula	NH_2-C_6H_4-CH_3
Melting temperature[a]	$T_m=243$ K
Glass transition[b]	$T_g\sim 187$ K
Mass density[c]	$\rho_m=[(1.225-8.1\times10^{-4}\ T(\mathrm{K})]\ 10^3$ kg m^{-3}
Sound velocity[d]	$c_a=[2723.5-3.85\ T(\mathrm{K})]$ m s^{-1}
Specific heat at constant pressure[e]	$C_p(T_g)=1.80\times10^3$ J kg^{-1} K^{-1}
Relative difference in specific heat at constant pressure[e]	$\nu_{C_P}(T_g)=0.44$
Relative difference in specific heat at constant volume[f]	$\nu_{C_V}(T_g)=0.38$
$\gamma=C_P^{\mathrm{th}}/C_V^{\mathrm{th}\ g}$	$\gamma=1.24$

[a]From [1(a)].
[b]From [1(b)].
[c]From [23].
[d]From [7].
[e]From [3].
[f]From [24].
[g]From Eqs. (2.6) and (2.2), and [3].

detection beams,[2] is shown for $T=330$ K in Fig. 1 for all the positive values of t. This figure illustrates, for $t\leqslant10^3$ ns, the decay of the phonons generated by the initial pulse and, for longer times, the decrease of the thermal grating due to the heat diffusion. More or less similar signals, recorded both in the VV geometry and in the HH geometry (i.e. for a polarization of the probe and detection beams parallel to the plane of the pump beams) and for several temperatures, are shown for times longer than 5 ns in Fig. 2. They exhibit the usual temperature evolution shown, e.g., in [9], and polarization changes similar to those already reported in [8].

Figure 1 also exhibits, around 10^3 ns, a sudden drop of the phonon signal which is not described by Eq. (1.2) because it is due to the finite length of the grating. This drop takes place when the lifetime of the phonons is of the order of, or longer than, the time a phonon takes to travel through this grating [10]. In our *m*-toluidine experiments, this drop is visible when the temperature is higher than 280 K (c.f. Fig. 1) or lower than 200 K. For such temperatures, we have not analyzed the corresponding 1–3 μs time interval.

The VV and HH signals were recorded from 330 K ($1.75T_g$) down to 190 K ($1.01T_g$) at the 26 temperatures listed in Tables III–V. At each temperature, the VV signal is negative for times up to a few ns, as exemplified in Fig. 1. This negative part is mostly due to the molecular OKE contribution, Eq. (2.9a) of Paper I, and to a much shorter intramolecular vibration contribution [11]. The duration of this OKE signal is shorter than but not negligible with respect to the characteristic time of the resolution function of the instrument, $F(t)$. The latter presents an important and broad first maximum at $t_a=1.40$ ns, followed by strongly damped oscillations with a short period of approximately 1.7 ns. Its precise description and an analytical approximation of this function are given in the attached EPAPS document [24] in Sec. A-1. As the accuracy of the apparatus does not allow us to know exactly the time at which the pumps start to act, we have fixed the time origin, $t=0$, of all the measurements by deciding that the first minimum of any $S_{\mathrm{VV}}^{\mathrm{expt}}(\vec{q},t)$ signal would take place at the time $t=t_a$ whatever the temperature. This implies that the pumps start to act at the unknown time $t=-t_0$ which varies with temperature because the molecular OKE signal is temperature dependent. The time t_0 will thus be one of our fit parameters; it actually varies around 0.45 ns. Also, as these short times negative contributions are not included in Eq. (1.2), they can simply serve to determine t_a at each temperature; the signals can be fitted only for times longer than 5 ns where the preceding contributions are totally negligible.

Figure 1 also shows that, for $T=330$ K, the VV signal still has negative parts in the 3–50 ns time interval. These parts can only arise from the ISBS contribution: the signals partly originate from the electrostrictive source.

B. Fixing the value of some *m*-toluidine parameters

Some of the experiments on *m*-toluidine listed in the Introduction have allowed us to fix the value and the thermal variation of different parameters that enter into Eqs. (1.2)–(1.4). This information is necessary for reducing, in Sec. III, the number of fits parameters in the data analysis. More precisely:

(1) $c_a(T)$ has been measured in [7] by an ultrasonic technique from 300 to 250 K (see Table I that summarizes the values of different parameters of *m*-toluidine); following that reference, we shall extrapolate its thermal dependence down to T_g.

(2) The rotational relaxation dynamics, long time part of $\Gamma(t)\equiv\Gamma^0 g_R(t/\tau_R)$, see Eq. (2.3b) of Paper I, was studied in

[2]In our experiments, the two pump beams were always polarized along V, i.e. perpendicular to the plane they define.

the same paper from 300 to 189 K by a combination of different techniques. Assuming that $\omega g_R(\omega\tau_R)$ could be described by a Cole-Davidson function,[3]

$$\omega g_R(\omega\tau_R) = 1 - \left(\frac{1}{1+i\omega\tau_R}\right)^{\beta_R}, \tag{2.1}$$

this experiment determined the thermal variations of τ_R and β_R.

(3) The *m*-toluidine Brillouin spectrum was also measured in [7], in a backscattering experiment. It was analyzed in the adiabatic approximation, see Eq. (1.4), and with a temperature independent value of $\bar{\gamma}$, $\bar{\gamma}(T_0)$, deduced from the Brillouin spectrum measured at $T_0=175$ K. Assuming for $\omega g_L(\omega\tau_L)$ the same stretching coefficient as for $\omega g_R(\omega\tau_R)$ $[\beta_L(T)=\beta_R(T)]$ and the same Cole-Davidson form, $\Delta_L(T)$ was derived in the whole temperature range. These $c_a(T)$ and $\Delta_L(T)$ values will be used for the fits of $S_{\rm iso}^{\rm expt}(\vec{q},t)$ while we shall write, following [12],

$$\bar{\gamma}(T) = \bar{\gamma}(T_0)\frac{T}{175}. \tag{2.2}$$

We also determined $\nu_{C_V}(T)$ from earlier measurements. Above 215 K, the fits of $S_{\rm iso}^{\rm expt}(\vec{q},t)$ will be performed in the adiabatic approximation of $P_L(\vec{q},\omega)$. As explained in Sec. A-2 of the attached EPAPS document [24], $\nu_{C_V}(T)$ is expressed, in this case, by

$$\nu_{C_V}(T) = \left(2 - \frac{T}{T_g}\right)\nu_{C_P}(T_g), \tag{2.3}$$

where $\nu_{C_P}(T_g)$ is obtained from Carpentier *et al.* [3]. Below 215 K, our fits will require the use of the isothermal form of $P_L(\vec{q},\omega)$. The more complex procedure necessary to obtain $\nu_{C_V}(T)$ when γ is different from unity is explained in Sec. A-2 of Ref. [24] and requires the knowledge of γ. The latter is obtained from

$$\gamma - 1 = T\frac{(\alpha^{\rm th})^2 c_a^2}{\rho_m^{-1}\gamma C_V^{\rm th}}, \tag{2.4}$$

where $\alpha^{\rm th}$ is the thermal expansion coefficient at constant pressure and $\rho_m^{-1}\gamma C_V^{\rm th}$ the specific heat at constant pressure per unit of mass, as obtained in a quasi-static measurement. All the quantities entering the right-hand side of Eq. (2.4) are known at T_g (see Table I) while we neglected the thermal dependence of γ and ν_{C_V} between 215 and 190 K.

III. FIT OF THE ISOTROPIC AND ANISOTROPIC SIGNALS

A. Introduction

This section describes the fit of $S_{\rm iso}^{\rm expt}(\vec{q},t)$ and $S_{\rm aniso}^{\rm expt}(\vec{q},t)$, the linear combinations of $S_{\rm VV}^{\rm expt}(\vec{q},t)$ and $S_{\rm HH}^{\rm expt}(\vec{q},t)$ defined in Eqs. (3.1) of Paper I, with Eqs. (1.1), (1.2), and (1.6). Those fits have been performed in the time space: we have looked

[3]Or the equivalent Kohlrausch function.

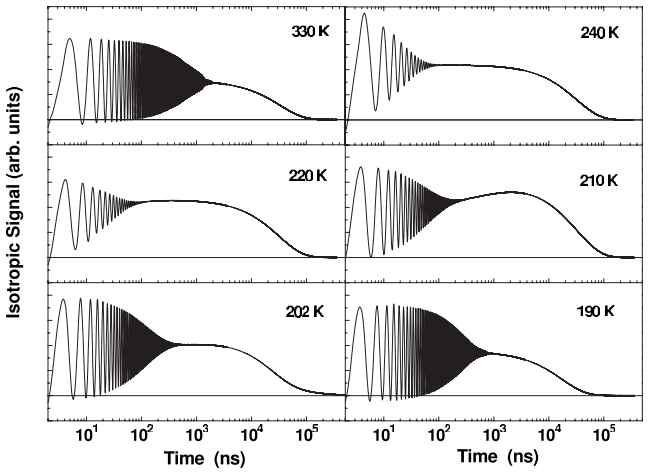

FIG. 3. $S_{\rm iso}^{\rm expt}(\vec{q},T)$ for the six same temperatures as in Fig. 2.

for the parameters that minimize $\Sigma_i[S_\alpha^{\rm expt}(\vec{q},t_i) - S_\alpha(\vec{q},t_i)]^2$ where data points for one value of t_i out of 12 were used for times shorter than 4 μs, all the data points being considered for longer times. Reliable inverse Laplace transfoms, $S_\alpha(\vec{q},t_i)$, were obtained for times t_i spanning a dynamical range larger than 10^5. Details on the corresponding program are given in Sec. A-3 of the attached EPAPS document [24]. All the different $\omega g_i(\omega\tau_i)$ were described by Cole-Davidson functions: each was characterized by its relaxation time, τ_i, and its stretching coefficient, β_i.

B. Fit of $S_{\rm iso}^{\rm expt}(\vec{q},t)$

Some "iso" spectra are shown in Fig. 3 for the same temperatures as in Fig. 2. Fits performed in the different temperature domains, with their corresponding approximations, are summarized in Table II. The quantities $c_a(T)$, $\Delta_L(T)$, $\bar{\gamma}(T)$, and $\nu_{C_V}(T)$ entering into Eqs. (1.3) and (1.4) having been determined in Sec. II, the number of fit parameters was further reduced by making the approximations $\tau_L=\tau_{C_V}=\tau_\beta$ and $\beta_{C_V}=\beta_\beta$.

1. Determination of a_0, the relative ISBS contribution to $S_{\rm iso}^{\rm expt}(\vec{q},t)$

The parameter a_0 measures the relative ISBS contribution to the signal, and t_0 is the time at which the pumps start to act. Both parameters should be correlated in the fitting procedure because the ISBS and ISTS contributions are both oscillatory at short times, with the same period but with a $\frac{\pi}{2}$ shift between them: an erroneous determination of a_0 can be partly compensated by a change of t_0 without affecting the quality of the fit.

To minimize this effect, we performed an initial fit in which both a_0 and t_0 were fit parameters. Though the quality of this fit was rather poor, it was sufficient to ascertain the anticipated correlation between t_0 and a_0, the latter randomly fluctuating between 10^{-5} and 2×10^{-5}. Assuming a_0 to be temperature independent, we fixed it at its mean value, 1.5×10^{-5}, which was then kept unchanged in all the subsequent fits.

TABLE II. Summary of the fits performed in Sec. III.

Name of the fit	Temperature range (K)	Fixed parameters	Fit parameters (I_{iso}, t_0)	Remarks
F_1	330–260	a_0, c_a, Δ_L, β_L, $\bar{\gamma}$	τ_L, τ_h^0	$\nu_{C_V}=\nu_\beta=0$
F_2	250–215	a_0, c_a, Δ_L, $\bar{\gamma}$, ν_{C_V}	τ_L, β_L, ν_β, τ_h^0	Adiabatic propagator $\beta_{C_V}=\beta_\beta=1$ $\tau_{C_V}=\tau_\beta=\tau_L$
F_3	212–190	a_0, c_a, Δ_L, $\bar{\gamma}$, ν_{C_V}	τ_L, β_L, ν_β, τ_h^0	Isothermal propagator $t>1$ μs $\beta_{C_V}=\beta_\beta=1.5\beta_L$ $\tau_{C_V}=\tau_\beta=\tau_L$
F_4	215–190	a_0, c_a, Δ_L, $\bar{\gamma}$, ν_{C_V}, ν_β, τ_h^0, τ_L	τ_L^s, β_L^s	Adiabatic propagator $t<1$ μs $\beta_{C_V}=\beta_\beta=1$ $\tau_{C_V}=\tau_\beta=\tau_L$
F_5	225–200	a_0, c_a, Δ_L, $\bar{\gamma}$, ν_{C_V}, ν_β, τ_L, β_L, τ_h^0	τ_μ, β_μ	Anisotropic spectrum $\beta_{C_V}=\beta_\beta=1$ $\tau_{C_V}=\tau_\beta=\tau_L$

2. The high temperature domain, 330 K ≥ T > 260 K

In this temperature domain, τ_L is so short with respect to the inverse of the phonon frequency that the signals contain little information; most aspects of the relaxation processes have to be neglected: $\omega g_L(\omega\tau_L)$ has to be approximated by its lowest term in ω, $i\omega\beta_L\tau_L$, $\beta_L(T)$ has to be taken equal to $\beta_R(T)$ measured in [7], while $\nu_{C_V}\omega g_{C_V}(\omega\tau_{C_V})$ and $\nu_\beta\omega g_\beta(\omega\tau_\beta)$ play a negligible role, see Eqs. (1.3) and (1.4). The fit is thus performed assuming $P_L^{-1}(\vec{q},\omega)$ to be written as

$$P_L^{-1}(\vec{q},\omega)=\omega^2-q^2(c_a^2+i\omega\gamma_1) \tag{3.1}$$

with

$$\gamma_1=\bar{\gamma}+\beta_L\Delta_L^2\tau_L, \tag{3.2}$$

while the bracket of Eq. (1.2) simplifies into

$$\frac{1}{1+i\omega\tau_h^0}-ia_0. \tag{3.3}$$

The values of the two physically meaningful parameters, τ_h^0 and τ_L, deduced from this fit F_1 are given in Table III. τ_h^0 is constant within 1.5%, which represents the fit accuracy, while the accuracy on τ_L will be discussed in Sec. IV C 1.

TABLE III. Parameters derived from the fit F_1. See Sec. IV C 1 for the accuracy of τ_L.

T (K)	τ_L (ns)	τ_h^0 (μs)
330	7×10^{-3}	32.6
320	8×10^{-3}	32.6
310	9×10^{-3}	32.5
300	1.0×10^{-2}	32.6
290	1.2×10^{-2}	32.7
280	1.7×10^{-2}	32.6
270	2.6×10^{-2}	32.6
260	5.3×10^{-2}	33.0

3. The medium temperature domain, 260 K > T ≥ 215 K

The fit F_2 is performed using the full adiabatic form of $P_L^{-1}(\vec{q},\omega)$. It determines the four parameters τ_L, τ_h^0, β_L, and ν_β, while the two other stretching parameters, β_β and β_{C_V}, have been fixed to unity (Debye relaxation functions).

Good quality fits are obtained at every temperature and the parameters have a smooth temperature variation (see Table IV). Two important results obtained in this domain are the continuous decrease of β_L from 0.31 at 250 K to 0.20 at 215 K and the continuous increase of τ_L up to a $\tau_L(T=215\text{ K})$ value of ≈1 μs, which approximately corresponds to the time when the phonon part of $S_{iso}^{expt}(\vec{q},t)$ has totally disappeared, see Fig. 3.

TABLE IV. Parameters derived from the fit F_2.

T (K)	τ_L (ns)	β_L	τ_h^0 (μs)	ν_β
250	0.19	0.31	32.4	0[a]
245	0.33	0.29	32.1	0[a]
240	0.61	0.27	32.2	0[a]
235	1.2	0.25	32.2	0.37
230	3.3	0.24	32.2	0.40
225	13	0.23	32.1	0.43
222.5	29	0.22	31.8	0.42
220	63	0.21	32.0	0.40
218	125	0.20	31.6	0.39
215	340	0.20	31.6	0.39

[a]Fixed to $\nu_\beta=0$ for those three temperatures, as well as for $T>250$ K.

TABLE V. First four columns: parameters derived from the fit F_3 (long time signal, $t>1$ μs). Last two columns: parameters derived from the fit F_4 (short time signal, $t<1$ μs). See Sec. IV C 1 for the accuracy of τ_L.

T (K)	τ_L (ns)	β_L	τ_h^0 (μs)	ν_β	τ_L^s (ns)	β_L^s
212	1.3×10^3	0.20	31.6	0.435	1.1×10^3	0.18
210	2.1×10^3	0.20	31.6	0.45	3.1×10^3	0.16
208	2.8×10^3	0.20	34.4	0.45	1.1×10^4	0.16
205	2.3×10^4	0.20	29.7	0.45	2.8×10^6	0.11
202	3×10^5	0.20	31.5	0.45	1.7×10^8	0.09
200	2×10^6	0.20	33.6	0.45	8.6×10^8	0.09
195	3×10^7	0.20	30.7	0.45	3.5×10^{10}	0.09
190	1×10^8	0.20	29.3	0.45		

4. Low temperature domain, 215 K$>T\geqslant$190 K; the long time, $t>1$ μs, signal

Below 215 K, the hypotheses used in the fit F_2 yield results of poorer and poorer quality as the temperature decreases down to 205–202 K and those fits remain unsatisfactory below that temperature. Substituting the Cole-Davidson description of $\omega g_L(\omega\tau_L)$ by ω times the LT of a Kohlrausch function did not substantially improve the quality of these fits and/or produced good fits but with unrealistic parameters.

The main source of this failure is that a Cole-Davidson form of $\omega g_L(\omega\tau_L)$ describes only the α part of a relaxation process. The use of such a function is reasonable when τ_L is shorter than the total duration of the phonon signal; in such a case, fast relaxation processes play very little role in the phonon decay detected in a HD-TG experiment while the remaining part of the signal is solely governed by the heat diffusion process. Conversely, below 215 K ($\approx 1.15T_g$), where τ_L becomes longer than 1 μs, the $t>1$ μs part of $S_{\rm iso}^{\rm expt}(\vec{q},t)$ reflects simultaneously the adjustment of $\delta\rho(\vec{r},t)$, through the "longitudinal" α-relaxation process, towards the value imposed by the local temperature, $\delta T(\vec{r},t)$, and the decay of this temperature modulation through the heat diffusion process. Meanwhile, the decay of the phonon part of $S_{\rm iso}^{\rm exp\,t}(\vec{q},t)$ is governed by the anharmonic term, $i\omega\bar{\gamma}(T)$, and by the short time part [or fast process(es) part] of the relaxation function. There is presently no theory that provides a reliable expression for those fast processes for temperatures below[4] $T\approx 1.2T_g$. We have thus divided the fit of $S_{\rm iso}^{\rm expt}(\vec{q},t)$ into two parts that correspond to the two time regions, $t>1$ μs (long times region) and $t<1$ μs (short times region).

We have started by fitting the first region where the effect of the fast relaxation processes is negligible. Good fits and meaningful fit parameters are obtained by

(a) stretching the relaxation processes of $C_V(\omega)$ and $\beta(\omega)$; $\beta_{C_V}=\beta_\beta=1.5\beta_L$ was found to be a reasonable choice; and

[4]This is a good order of magnitude for the critical temperature, T_c, of the mode coupling theory [13].

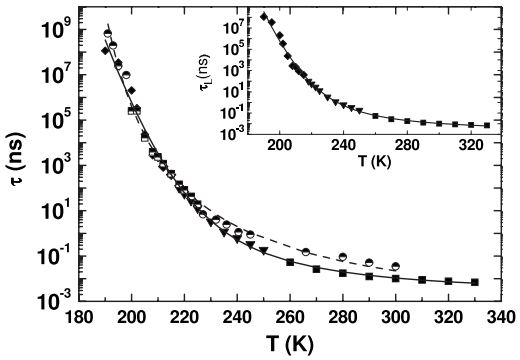

FIG. 4. The "longitudinal" relaxation time, τ_L, versus temperature, deduced from the fits F_1 (330 K$\geqslant T\geqslant$260 K) (■), F_2 (260 K$>T\geqslant$215 K) (▼), and F_3 (215 K$>T\geqslant$190 K, $t>1$ μs) (◆), and its fit with the four parameters expression Eq. (4.2), (—). Also represented are the rotational relaxation time, τ_R (◓) with its Vogel Fulcher interpolation [7] (----), and the translation-rotation relaxation time, τ_μ (⬒). The inset shows in more details the part of the figure related to τ_L.

(b) making use of the isothermal form of the phonon propagator ($\gamma\neq 1$) so that the heat diffusion time, $\bar{\tau}_h^0=\gamma\tau_h^0$ [see Eq. (3.14) of Paper I], is larger than τ_h^0.

The parameters corresponding to this fit, F_3, are reported in Table V where one notes the quasi independence of β_L and ν_β on temperature. Figures 4 and 5 show the values of τ_L and $\bar{\tau}_h^0$ obtained through the three fits F_1, F_2, and F_3, i.e., in the whole temperature range covered by our experiments.

5. Low temperature domain, 215 K$>T\geqslant$190 K; the short time, $t<1$ μs, signal

No analytical form being known for the fast relaxation processes in this temperature range, we mimicked it by another Cole-Davidson function which replaces, in Eq. (1.4), the α-relaxation process. Thus in the fit, F_4, of the short time ($t<1$ μs) part of the spectrum, we used the same adiabatic phonon propagator and the same values, $\beta_{C_V}=\beta_\beta=1$, as in

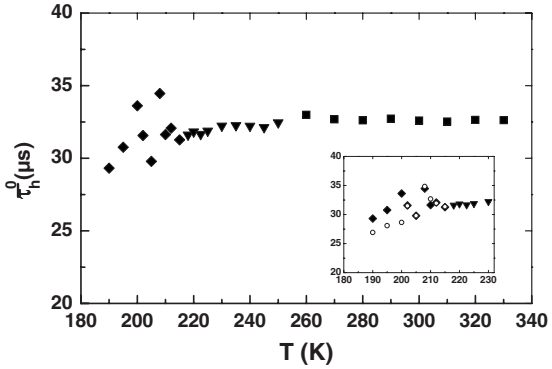

FIG. 5. The heat diffusion time, $\bar{\tau}_h^0$, versus temperature, deduced from the fits F_1 (330 K$\geqslant T\geqslant$260 K) (■), F_2 (260 K$>T\geqslant$215 K) (▼), and F_3 (215 K$>T\geqslant$190 K, $T<1$ μs) (◆). The inset compares, for $T\leqslant$215 K, the values of $\bar{\tau}_h^0$ deduced from the isothermal description of the phonon propagator (◆) and from its adiabatic approximation (○).

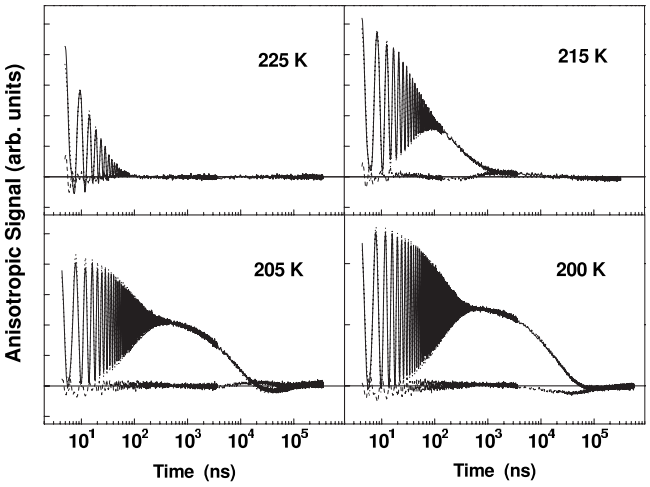

FIG. 6. $S^{\text{expt}}_{\text{aniso}}(\vec{q},T)$ at four different temperatures (–). The difference spectrum, $S^{\text{expt}}_{\text{aniso}}(\vec{q},T)-S_{\text{aniso}}(\vec{q},T)$ (···) is also reported.

the fit F_2 while ν_β and τ_h^0 took the values determined in F_3. The corresponding parameters, τ_L^s and β_L^s, are given in the two last columns of Table V and they lead to quite good quality fits. The consistency between the results of F_3 and F_4 will be discussed in Sec. IV C 3.

C. Fit of the anisotropic signal

$S^{\text{expt}}_{\text{aniso}}(\vec{q},t)$ is shown in Fig. 6 for four temperatures ($T<230$ K) at which its value is not negligible and has been fitted, at each temperature, with Eq. (1.6). Its use requires the knowledge of a single function $S_{\text{iso}}(\vec{q},\omega)$ that provides a good fit to $S^{\text{expt}}_{\text{iso}}(\vec{q},t)$ for the whole time range. Most of the $S^{\text{expt}}_{\text{aniso}}(\vec{q},t)$ signals correspond to temperatures below 215 K where the fits of Sec. III B did not determine such a function. We thus proceeded, for those temperatures, to an intermediate fit, similar to F_2, but in which $c_a(T)$ was no longer imposed. As expected, the fit was quite good over the whole time range but with unphysical values for some parameters. Using this representation of $S_{\text{iso}}(\vec{q},\omega)$, a good fit, F_5, of $S^{\text{expt}}_{\text{aniso}}(\vec{q},t)$ is obtained at each temperature, as also shown in Fig. 6 where both this signal and the difference signal, $S^{\text{expt}}_{\text{aniso}}(\vec{q},t)-S_{\text{aniso}}(\vec{q},t)$, are represented. F_5 gives, on top of the parameters τ_μ and β_μ, the value of K_{aniso}, which is found to be temperature independent and approximately equal to 0.12.

IV. DISCUSSION

A. Introduction

The analysis of our HD-TG experiment on *m*-toluidine has made use of three ingredients that had not been included in the seminal work of Yang and Nelson [14].

(1) the phenomena that appear when the supercooled liquid is formed of anisotropic molecules;

(2) the possibility of comparing the experimental signals with a theoretical formulation expressed in the frequency space, through the use of a numerical inverse Laplace transform technique; and

(3) the frequency dependence of some ingredients of the theory: specific heat and tension coefficient.

In this final section we successively discuss [15] the information we have obtained through the introduction of these aspects on

(1) the dynamics of the anisotropic signal and the contribution of the molecular channel to the recorded signals (Sec. IV B);

(2) the dynamics of the longitudinal phonons (Sec. IV C); and

(3) the influence of the various relaxation processes on the decay of the thermal grating (Sec. IV D).

This section will end with a brief comparison with the results that would result from a Yang-Nelson type of analysis of this experiment and with some remarks on the use of the present method for the study of other glassforming liquids.

B. The anisotropy channel

1. The translation-rotation relaxation function

The relaxation time, $\tau_\mu(T)$, determined in Sec. III C, is shown in Fig. 4 for the temperature range 225–200 K where it has been safely determined. This figure also shows the rotational time $\tau_R(T)$ obtained in [7], with its Vogel-Fulcher interpolation at intermediate temperatures: the agreement between τ_μ and the interpolated values of τ_R is very good. Though still reasonable, this agreement is less convincing for the stretching coefficients: $\beta_R(T)$ ranges from 0.4 ($T=225$ K) to 0.33 ($T=203$ K) [16] while $\beta_\mu(T)$ can be fixed, with a rather poor accuracy, at the somewhat higher value $\beta_\mu=0.45\pm0.1$ in the same temperature range.

A close similarity between $\Gamma(t)=\Gamma^0 g_R(t/\tau_R)$, see Sec. II, and $\mu(t)\propto g_\mu(t/\tau_\mu)$ had been previously postulated, whatever the temperature, for both *m*-toluidine [17] and salol [12]. The present study brings information on that hypothesis and supports its validity.

2. Relative importance of the anisotropy channel

K_{aniso} can be expressed, see Eq. (3.9b) of Paper I, as

$$K_{\text{aniso}}=\lim_{\omega\tau_\mu\to\infty}\left(\frac{\Lambda'}{\rho_m}\frac{b}{a}r(\omega)\right), \tag{4.1}$$

where the quantity inside the bracket is the relative contribution of the molecular channel with respect to the mass density channel, both as a source and as a detection mechanism, cf. Eq. (2.9c) of Paper I. $K_{\text{aniso}}=0.12$, as obtained in Sec. III C, indicates that this relative contribution is small but not negligible. Furthermore, one can also evaluate the relative contributions of electrostriction (change in mass density) and heat absorption on the initial formation of the grating. With $a_0=1.5\times10^{-5}$, this ratio is of the order of 0.20 for the Nd-YAG laser used here for the pumps. These two numbers confirm our qualitative findings: the molecular channel is

negligible as a source of the grating but must be taken into account as a detection mechanism.

C. The "longitudinal" relaxation function, $g_L(t/\tau_L)$

1. The α relaxation time, τ_L

On top of $\tau_L(T)$ determined in the fits F_1, F_2, and F_3, the inset of Fig. 4 represents the fit of this relaxation time by the four parameters expression [18]

$$\log_{10}(\tau_L) = \log_{10}(\tau^0) + A/[(T - T^0) + \sqrt{(T - T^0)^2 + BT}], \tag{4.2}$$

with $\log_{10}(\tau^0) = -2.85$, $A = 143.1$ K, $T^0 = 223.2$ K, and $B = 5.23$ K. This expression generalizes the usual Vogel-Fulcher formula. The values of τ_L cover approximately a 10^{10} dynamical range and correspond to the whole temperature range of our measurements. Yet, the accuracy of the reported values varies with temperature and needs to be discussed.

Between 330 and 270 K, Table III, τ_L was deduced from the damping term γ_1, see Eq. (3.2) that we repeat here:

$$\gamma_1 = \bar{\gamma} + \beta_L \Delta_L^2 \tau_L. \tag{4.3}$$

The inaccuracy on τ_L results only from those on $\bar{\gamma}$, β_L, and Δ_L. Those are large enough to yield a final uncertainty of the order of a factor 1.5 at the highest temperatures, this factor decreasing with decreasing temperature. This is only partly reflected in the numerical values of Table III in order to represent the better accuracy existing on the thermal variation of τ_L.

The inset of Fig. 4 also exhibits a clear underestimation of τ_L at 190 K as well as smaller inaccuracies at 195 and 200 K that are apparent when comparing the individual data to their four parameter fit. Factors of 3–5 are possible for the values obtained at those three temperatures but not on the fit. The latter has accuracy close to 2, even for the lowest temperatures of Table V.

Figure 4 provides a comparison between the temperature variations of τ_L and τ_R. It exhibits a trend already found by Zhang *et al.* [12] in salol: the ratio τ_R/τ_L tends to increase with increasing temperature, in particular in the region $1.2T_g - 1.4T_g$ where this would not be predicted by the mode coupling theory [13]. In this temperature interval, this ratio increases by a factor of 2 in *m*-toluidine and by a factor of 4 in salol.

2. The stretching coefficient, β_L

β_L could be determined only from 250 K ($\beta_L = 0.31$) to 195 K ($\beta_L = 0.20$), its value remaining constant below 220 K. Such low values contrast with those reported in Sec. IV B 1 for β_μ and β_R but are in line with values recently reported for other longitudinal phonon propagators in molecular supercooled liquids in the same relative temperature range and with the same Cole-Davidson description of the relaxation process. For instance, Comez *et al.* [19] report $\beta_L = 0.27$ in glycerol, and Zhang *et al.* [12] a value lower than $\beta_L = 0.2$ in salol. Higher values seem typical of other variables. For instance, a systematic difference seems to exist between β_L and β_d, the stretching coefficient obtained in dielectric spectroscopy. The latter probes the correlation function of the local dipole moment, a quantity not related to the variables studied here: one finds for the supercooled liquids just mentioned, β_d values respectively equal to 0.30 at $T_g - 0.42$ at $1.2T_g$ (*m*-toluidine [3]), 0.52 at $T_g - 0.62$ at $1.2T_g$ (glycerol [20]), and 0.40 at $T_g - 0.53$ at $1.2T_g$ (salol [21]).

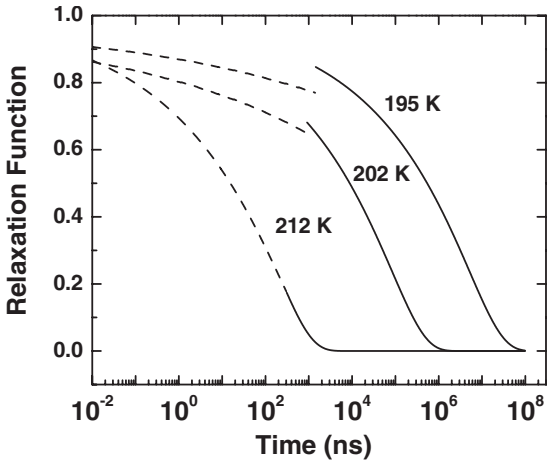

FIG. 7. The short time (--) and long time (–) parts of the total "longitudinal" relaxation functions, LT^{-1} $[g_L(\omega\tau_L)]$, for three temperatures below 215 K.

3. The fast and the α-relaxation processes

Table V also gives the values of τ_L^s and β_L^s which have been found to describe best the "fast relaxation" part of the longitudinal relaxation dynamics for times shorter than 0.5–1 μs. They contrast with the τ_L and β_L values shown in Table V, which characterize the α-relaxation part of the same process. If a unique analytical expression, $g_L(t/\tau_L)$, could have been obtained for those two time domains, one would have expected it to have approximately the shape proposed by the mode coupling theory [13] at higher temperatures ($T > T_c$). It should start, at very short times, at a value smaller than unity and slowly decrease, on a logarithmic scale, as long as t has not passed from the "fast" to the α-relaxation process. At longer times, this function should have a more rapid decrease on this logarithmic scale. The composite functions represented in Fig. 7 are made of the two functions which generate, in the frequency space, the corresponding Cole-Davidson functions. For each temperature, the anticipated behavior is approximately obtained.

D. Discussion of the final decay of the isotropic signal; thermal variation of $\bar{\tau}_h^0$

Different factors contribute to the final decay of the isotropic signal. Their role can be understood through the study of $\bar{\tau}_h^0$. By definition, see Paper I,

$$\bar{\tau}_h^0 = \frac{C_P^{\text{th}}}{\lambda q^2}, \tag{4.4}$$

where λ is the heat diffusion coefficient: one thus expects $\bar{\tau}_h^0$ to be only weakly temperature dependent with a monotonic

variation. The thermal variation determined through our fits is shown in Fig. 5. Down to 210 K, it has no thermal variation within 1.5%, which corresponds to the fit uncertainty. Below that temperature, it still remains approximately constant though it exhibits larger inaccuracies whose origin we discuss now.

The time rate, τ_{eff}, at which $S_{\text{iso}}(\vec{q},t)$ decreases in the 10–100 μs region is approximately equal to, see Eq. (1.2),

$$\tau_{\text{eff}} = \tau_h\left(\vec{q}, \omega = \frac{1}{\tau_h^0}\right), \tag{4.5}$$

where $\tau_h(\vec{q},\omega)$ is given by Eq. (1.3). For temperatures for which $\tau_L < \tau_h^0$, the value of $\omega g_{C_V}(\omega\tau_{C_V})$ is negligible for $\omega \approx (\tau_h^0)^{-1}$ and the frequency dependence of $C_V(\omega)$ does not show up in the final decay of the signal. This is no longer the case when $\tau_L > \tau_h^0$: $\omega g_{C_V}(\omega\tau_{C_V})$ has a finite value in the same frequency range and τ_{eff} decreases by a factor of the order of $1-\nu_{C_V}$ when the temperature tends towards T_g. Ignoring the frequency dependence of $C_V(\omega)$ in $\tau_h(\vec{q},\omega)$ would result in a fit value of τ_h^0 equal to τ_{eff} so that $\bar{\tau}_h^0$ would decrease with temperature below 210 K, by a factor close to 2 in the present case.

Also, the fits performed in Sec. III B 4 have shown that good fits of $S_{\text{iso}}^{\text{expt}}(\vec{q},t)$ for temperatures lower than 212 K require that one takes into account the role of the adiabatic-isotherm correction, last term of Eq. (1.4). The inset of Fig. 5 compares the values of $\bar{\tau}_h^0$ obtained between 190 and 215 K, without and with the inclusion of that correction. The latter brings a noticeable improvement at the three lowest temperatures. However, the 8% remaining fluctuations on $\bar{\tau}_h^0$ for temperatures below 212 K do not result from meaningless correlations between parameters: smoothing $\bar{\tau}_h^0$ at its mean value between 212 and 195 K yields, for some temperatures, fits of lower qualities and produces higher fluctuations on $\tau_L(T)$. This is not surprising: the series of assumptions $\tau_{C_V}=\tau_\beta=\tau_L$, $\beta_{C_V}=\beta_\beta=p\beta_L$, where the $p=1.5$ value has been fixed by a trial and error process, have no other justification than simplicity. Unfortunately, we have presently no additional measurements, such as the frequency dependence of the thermal expansion coefficient at constant pressure, $\alpha(\omega)$, or of the shear viscosity, $\omega\eta_s(\omega)$, at temperatures close to T_g which would allow us to fix more parameters and decrease the number of unsubstantiated approximations.

Let us nevertheless note that this HD-TG experiment gives the first proof of the existence of a frequency dependence of the tension coefficient, $\beta(\omega)$. Though the accuracy on $\nu_\beta(T)$ is not very good ($\approx$20%), we have found by arbitrarily varying the value of ν_{C_V} at a given temperature that there is a strong correlation between ν_{C_V} and ν_β. The nonzero value of $\nu_{C_V}(T)$ requires that ν_β also differs from zero in the whole temperature range covered by our experiments.

E. Comparison with the Yang-Nelson technique and perspective for future work

Yang and Nelson [14] proposed to represent the ISTS and ISBS contribution to the "iso" signal detected through the mass density fluctuations by

$$R^2(\vec{q},t) = A[\exp(-t/\tau'_h) - \exp(-\Gamma_B t)\cos(\omega_B t)] + B[\exp(-t/\tau'_h) - \exp(-(t/\tau'_L)^{\beta'_L})], \tag{4.6}$$

$$R^3(\vec{q},t) = C\exp(-\Gamma_B t)\sin(\omega_B t), \tag{4.7}$$

where $\omega_B/2\pi$ and $\Gamma_B = 1/\tau_B$ are the apparent phonon frequency and damping constant, τ'_h the apparent heat diffusion constant, while τ'_L and β'_L characterize the α-relaxation process, all these quantities being fit parameters.

The most recent efforts to use this approach for a supercooled molecular liquid were made by Torre *et al.* [9] on *o*-TP. They found that they could determine safely τ'_L only in the region where this time is longer than the phonon lifetime and shorter than τ'_h; this represents a 10^3 dynamical range. The present method, which compares the signal with an analytical formulation of the problem, has allowed us to obtain information on τ_L in a much wider dynamical range, even if the corresponding accuracy is not very good in the whole temperature range.

Also, the Yang and Nelson's method always yields β'_L values much larger than β_L obtained here or by light scattering methods in the same temperature range. This discrepancy arises from the fact that their method determines τ'_L in a time range where the stretching coefficient influences the $t > \tau'_L$ or $t \gg \tau'_L$ part of the stretched exponential. In this time region no comparison is possible between a stretched exponential and the function that gives rise to the Cole-Davidson function. Comparing β'_L and β_L is thus meaningless.

Finally, Eq. (4.6) ignores, by definition, the possible frequency dependence of $C_V(\omega)$. Apart from a small accident around the temperature at which $\tau'_h \approx \tau'_L$, see [22], τ'_h is approximately equal to τ_{eff} discussed in the preceding section. This parameter thus cannot have a smooth thermal variation, as recognized, e.g., in [9].

To conclude, let us stress that the results presented here could not have been obtained without the prior knowledge of other parameters and of their thermal variation. In particular, the use of both $c_a(T)$ and $\Delta_L(T)$ have been necessary to obtain reliable results. Also, our assumption on the independence of the coefficient a_0 (relative weights of the two detection channels) on temperature partly relies on the knowledge of $\rho_m(T)$, which suggests that $\beta^{\text{th}}(T)$, as $\alpha^{\text{th}}(T)$, has only a weak variation with temperature. Provided that those preliminary measurements have been performed, HD-TG is a valuable technique for a deeper study of supercooled liquids, which largely complements, for instance, the polarized Brillouin technique. In particular, most of the liquids studied so far by the TG technique have been fragile glass formers, for which the ratio $c_a(T)/\Delta(T)$ is usually smaller than unity. Stronger glass forming liquids, such as $ZnCl_2$ or diluted solutions of alkali halides, have a much higher ratio; they may reveal variations of the "longitudinal" relaxation time in the medium temperature range that could not be studied up to now. Also, the relationship between α^{th} and β^{th} suggests that thermal expansion anomalies of supercooled liquids could be revealed by the HD-TG technique and lead to new effects.

ACKNOWLEDGMENTS

This study has been made possible by Contract No. RII3-CT-506350 EC which allowed the French group to realize at LENS the experiments that form the basis of the present work and to discuss with the Italian group many issues related to its analysis. The latter has been made possible thanks to support from MENRT to A. A. and by additional support from the Université Franco Italienne which supported his one year stay at LENS. This work was also supported by CRS-INFM-Soft Matter (CNR) and MIUR-COFIN-2005 Grant No. 2005023141-003. We finally wish thank H. Z. Cummins for his constant help during the writing of this paper.

[1] (a) V. Legrand, M. Descamps, and C. Alba Simionesco, Thermochim. Acta **307**, 77 (1997); (b) C. Alba-Simionesco, J. Fan, and C. A. Angell, J. Chem. Phys. **110**, 5262 (1999).

[2] V. Legrand, Ph.D. thesis, Université de Lille, 1996 (unpublished).

[3] L. Carpentier, R. Decressain, and M. Descamps, J. Chem. Phys. **121**, 6470 (2004).

[4] R. Torre, P. Bartolini, M. Ricci, and R. M. Pick, Europhys. Lett. **52**, 324 (2000).

[5] R. Chelli, G. Cardini, P. Procacci, R. Righini, and S. Califano, J. Chem. Phys. **116**, 6205 (2002).

[6] R. Chelli, G. Cardini, P. Procacci, R. Righini, and S. Califano, J. Chem. Phys. **119**, 357 (2003).

[7] A. Aouadi, C. Dreyfus, M. Massot, R. M. Pick, T. Berger, W. Steffen, A. Patkowski, and C. Alba-Simionesco, J. Chem. Phys. **112**, 9860 (2000).

[8] A. Taschin, R. Torre, M. Ricci, M. Sampoli, C. Dreyfus, and R. M. Pick, Europhys. Lett. **56**, 407 (2001).

[9] R. Torre, A. Taschin, and M. Sampoli, Phys. Rev. E **64**, 061504 (2001).

[10] A. Taschin, P. Bartolini, R. Eramo, and R. Torre, Phys. Rev. E **74**, 031502 (2006).

[11] P. Bartolini, M. Ricci, R. Torre, and R. Righini, J. Chem. Phys. **110**, 8653 (1999).

[12] H. P. Zhang, A. Brodin, H. C. Barshilia, G. Q. Shen, H. Z. Cummins, and R. M. Pick, Phys. Rev. E **70**, 011502 (2004).

[13] W. Götze, in *Liquids, Freezing and the Glass Transition*, edited by J. P. Hansen and D. Levesque (Plenum, New York, 1989), p. 287; W. Götze and L. Sjögren, Rep. Prog. Phys. **55**, 241 (1992), and references therein.

[14] Y. Yang and K. A. Nelson, J. Chem. Phys. **103**, 7722 (1995).

[15] A very brief report of some parts of this information has been published in A. Azzimani, C. Dreyfus, R. M. Pick, P. Bartolini, A. Taschin, and R. Torre, J. Phys.: Condens. Matter **19**, 205146 (2007).

[16] A. Aouadi (private communication).

[17] C. Dreyfus, A. Aouadi, R. M. Pick, T. Berger, A. Patkowski, and W. Steffen, Eur. Phys. J. B **9**, 401 (1999).

[18] M. H. Cohen and G. S. Grest, Phys. Rev. B **20**, 1077 (1979).

[19] L. Comez, D. Fioretto, F. Scarponi, and G. Monaco, J. Chem. Phys. **119**, 6032 (2003).

[20] K. L. Ngai, P. Lunckenheimer, C. Leon, U. Schneider, R. Brand, and A. Loidl, J. Chem. Phys. **115**, 1405 (2001).

[21] F. Stickel, E. W. Fischer, and R. Richert, J. Chem. Phys. **102**, 6251 (1995).

[22] R. M. Pick, C. Dreyfus, A. Azzimani, R. Gupta, R. Torre, A. Taschin, and T. Franosch, Eur. Phys. J. B **39**, 169 (2004).

[23] J. Timmermans, *Physico-Chemical Constants of Pure Organic Compound* (Elsevier, New York, 1950).

[24] See EPAPS Document No. E-PLEEE8-75-048705 for Sec. A-1: description of the response function of the LENS instrument; Sec. A-2: determinations of $\nu_{C_V}(T)$ in the case of the adiabatic approximation of the phonon propagator and in the case of its isothermal form; Sec. A-3: details on the inverse Laplace Transform program. For more information on EPAPS, see http://www.aip.org/pubservs/epaps.html.

[25] A. Azzimani, C. Dreyfus, R. M. Pick, P. Bartolini, A. Taschin, and R. Torre, preceding paper, Phys. Rev. E **76**, 011509 (2007).